Precision constraints on the neutron star equation of state with third-generation gravitational-wave observatories

Kris Walker,[1,2,*] Rory Smith,[3,†] Eric Thrane,[2,3] and Daniel J. Reardon[4,5]

[1]*International Centre for Radio Astronomy Research, University of Western Australia, 35 Stirling Highway, Crawley, Western Australia 6009, Australia*
[2]*OzGrav: The ARC Centre of Excellence for Gravitational Wave Discovery, Clayton, Victoria 3800, Australia*
[3]*School of Physics and Astronomy, Monash University, Victoria 3800, Australia*
[4]*Swinburne University of Technology, PO Box 218, Hawthorn, Victoria 3122, Australia*
[5]*OzGrav: The ARC Centre of Excellence for Gravitational Wave Discovery, Hawthorn, Victoria 3122, Australia*

(Received 5 January 2024; accepted 3 July 2024; published 6 August 2024)

It is currently unknown how matter behaves at the extreme densities found within the cores of neutron stars. Gravitational waves from binary neutron star mergers encode rich information about the stars' deformability, allowing the equation of state—and hence nuclear physics—to be inferred. Planned third-generation gravitational-wave observatories, having vastly improved sensitivity, are expected to provide tight constraints on the neutron star equation of state. We combine simulated observations of binary neutron star mergers by the third-generation observatories Cosmic Explorer and Einstein Telescope to determine future constraints on the equation of state across a plausible neutron star mass range. In one year of operation, a network consisting of one Cosmic Explorer and the Einstein Telescope is expected to detect $\gtrsim 3 \times 10^5$ binary neutron star mergers. By considering only the 75 loudest events, we show that such a network will be able to constrain the neutron star radius to at least $\lesssim 200$ m (90% credibility) in the mass range 1–1.97$M_\odot$—about ten times better than current constraints from LIGO-Virgo-KAGRA and NICER. The constraint is $\lesssim 75$ m (90% credibility) near 1.4–1.6$M_\odot$ where we assume the binary neutron star mass distribution is peaked. This constraint is driven primarily from the loudest $\sim$20 events.

DOI: 10.1103/PhysRevD.110.043013

I. INTRODUCTION

The cores of neutron stars host the densest baryonic matter in the Universe. Traveling from the neutron star surface down toward the core, it is conjectured that matter first forms a homogeneous neutron liquid before the appearance of strange baryons and/or deconfined quarks; see Ref. [1] for a review. Theoretical calculations of nuclear physics describing the interiors of neutron stars are notoriously difficult, and laboratory experiments do not begin to approach the necessary densities. Therefore, astronomical measurements of the neutron star equation of state provide a unique probe of nuclear physics at the most extreme possible densities.

Gravitational waves contain rich information about the tidal deformations experienced by coalescing neutron stars, encoding details about the mysterious physics of their interiors [2]. The susceptibility of a neutron star to deformation by tidal forces is determined by the equation of state of the material composing the star and is quantified by the dimensionless tidal deformability

$$\Lambda = \frac{2}{3} k_2 \left(\frac{c^2 R}{Gm}\right)^5. \tag{1}$$

Here, k_2 is the tidal Love number while m and R are the mass and radius of the star. The effects of deformations on the gravitational waveform are subtle. Nevertheless, current observations have ruled out some of the "stiffest" [3] proposed equations of state [4,5]. These constraints are expected to improve dramatically with the advent of third generation observatories such as Cosmic Explorer [6–8] and the Einstein Telescope [9–11], which aim to probe gravitational-wave strains more than an order of magnitude weaker than is possible with current observatories.

The precision to which the neutron star equation of state can be measured has been explored in a number of works in the context of second generation observatories [12–19]. In the first fully Bayesian analysis, the authors of [13] considered a linear approximation of $\Lambda(m)$ and found that a few tens of mock events observed by the Advanced LIGO-Virgo

*Contact author: kris.walker@icrar.org
†Contact author: rory.smith@ligo.org

network are sufficient to constrain the tidal deformability to 10% accuracy at a reference mass of $1.4M_\odot$. This work was extended in [15], which considered a piecewise polytropic parametrization of the equation of state and showed that—with a network of two Advanced LIGO and one Advanced VIRGO detectors—Λ can be constrained to 10%-50% accuracy across the mass range 1–$2M_\odot$. Reference [19] added additional realism, estimating the constraints available after the first 40 binary neutron star detections.

Some recent work has begun to establish the constraints that will be possible with third-generation observatories. Ref. [20] illustrates the ability of Cosmic Explorer or the Einstein Telescope to discriminate between equation of state models. Refs. [21,22] use Fisher matrix methods to predict constraints by third-generation observatories on the pressure and radius, respectively. Ref. [23] uses a Bayesian method to estimate the equation of state from simulated f-mode oscillations of isolated pulsars, while [24–26] similarly use Bayesian methods to estimate the equation of state from simulated binary neutron star mergers.

However, despite these predictions, computational difficulties have so far prevented a realistic analysis. Thus, previous work has resorted to approximate methods to deal with the high computational cost of inferring binary neutron star parameters from such long-duration signals. In particular, these analyses have either restricted to only the high-frequency part of the signal (e.g. [24,26]), or used Fisher matrix estimation to approximate the binary neutron star posterior distribution as a multivariate Gaussian (e.g. [21,22]). However, the former misses a significant amount of signal information, while the latter may not accurately describe the true distribution of some waveform parameters [27].

In this paper, we use reduced-order modeling [28] to perform the first realistic, fully Bayesian analysis of simulated long-duration (~12 min) gravitational waveforms from coalescing neutron stars—as observed by a network consisting of one Cosmic Explorer and one Einstein Telescope—to derive constraints on the neutron star equation of state across the full neutron star mass range.

We simulate the loudest binary neutron star events from one year of coincident data from the network. We consider Cosmic Explorer located at the site of LIGO Hanford, and the Einstein Telescope located at the site of Virgo [29], both with target specifications as described in [7]. For each event, we obtain measurements of the mass and tidal deformability. The dependence of the tidal deformability on the mass, $\Lambda(m)$, is uniquely determined by the equation of state through the Tolman-Oppenheimer-Volkoff equation. Using a spectral decomposition, we apply hierarchical inference to constrain the equation of state across the mass range 1–$1.97M_\odot$.

II. METHOD

Our first step is to generate a set of the 75 loudest binary neutron star mergers likely to be observed by an observatory array consisting of one Cosmic Explorer and one Einstein Telescope in one year of coincident data [7]. The merger distances are sampled from the neutron star merger rate density model given in [30], which is parametrized by the minimum merger timescale $t_{\rm min}$ and exponent α of the merger time distribution $\mathrm{d}N/\mathrm{d}t_{\rm merger} = t^\alpha$. While there is significant freedom in the choice of these parameters, the resulting difference in detection rate is insignificant in the case of Cosmic Explorer + Einstein Telescope at the low redshifts of the 75 loudest events. We therefore simply choose $t_{\rm min} = 10$ Myr and $\alpha = -1/2$. The other extrinsic parameters are drawn from standard distributions. In light of the low observed spins of neutron star binaries [31–33], we take all the neutron stars to have zero spin for simplicity (though we note that the presence of spin can have an effect on the inferred equation of state [34,35]). We sample the masses from a Gaussian approximation to the observed Galactic neutron star mass distribution [36], though, see Ref. [37]. For this analysis we assume an `SLy` equation of state [38], which determines the tidal deformabilities from the masses. For each event, we calculate the gravitational waveform using the `IMRPhenomPv2_NRTidal` approximant included in the LALSuite software suite [39]. The waveforms have a typical low-frequency cutoff of ~11 Hz, corresponding to an average signal duration of ~12 min.

To measure the equation of state from the mock events, we use the following procedure:

(1) We use the DYNESTY dynamic nested sampling package [40] included in BILBY [41–43] to perform Bayesian inference on each event i with data d_i. The priors are chosen to be the same distributions from which the mock binaries are sampled. We use the `ROQGravitationalWaveTransient` likelihood, which implements a reduced-order quadrature integration rule to greatly speed up evaluation [28,44]. This yields posterior distribution samples for the binary parameters, θ_i. For this investigation, we are interested only in the component masses m_1, m_2 and the tidal deformabilities Λ_1, Λ_2. We therefore marginalize over the other parameters to obtain the marginal posteriors, which are proportional to the marginal likelihoods $\mathcal{L}(d_i|m_1^i, m_2^i, \Lambda_1^i, \Lambda_2^i)$. An example is shown in Fig. 1. The distributions are highly non-Gaussian, making a Fisher matrix approximation inappropriate for analyzing these signals.

(2) As discussed in [19], it is necessary to interpolate between posterior samples in order to integrate the $\mathcal{L}(d_i|m_1^i, m_2^i, \Lambda_1^i, \Lambda_2^i)$ along the different equation-of-state curves. We therefore use a kernel density estimate (KDE)—calculated using an Epanechnikov kernel—to obtain a continuous representation of the marginal likelihood function [45].

(3) To obtain the marginal likelihood for the data given a particular equation of state, we integrate each

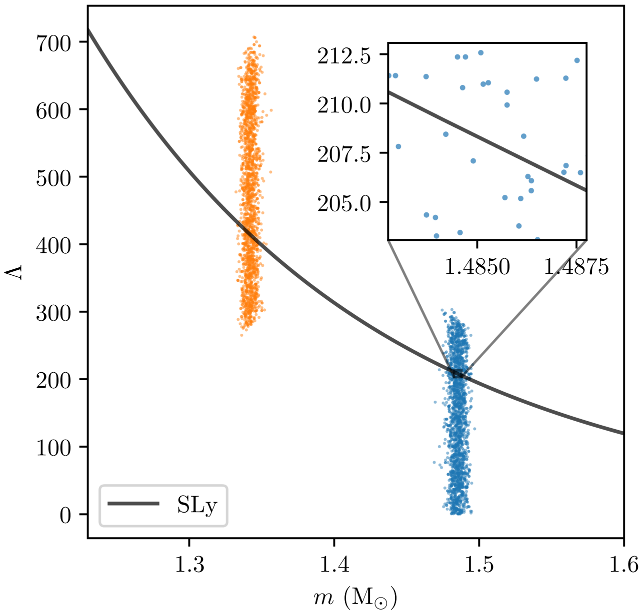

FIG. 1. The marginalized m-Λ posteriors (blue and orange points) from parameter estimation on a merger event overlayed on the black $\Lambda(m)$ curve predicted by the SLy equation of state. Because individual measurements produce a set of (zero-dimensional) discrete posterior samples, there is vanishingly small probability that any equation of state curve will pass through even a single posterior sample (see inset). We therefore estimate a continuous probability density from the samples that can be integrated along a curve passing through it.

$\mathcal{L}(d_i|m_1^i, m_2^i, \Lambda_1^i, \Lambda_2^i)$ along the predicted $\Lambda(m)$ curve and take their product to obtain the total likelihood.

To model the equation of state, we use a four-parameter spectral decomposition. In this representation, the adiabatic index is given as a function of the pressure p by

$$\Gamma(p) = \exp\left(\sum_{k=0}^{3} \gamma_k \ln(p/p_0)^k\right), \tag{2}$$

where $p_0 = 1.64 \times 10^{32}$ Pa is a reference pressure, and γ_k are coefficients determined by the equation of state. The equation of state (energy density as a function of pressure) $\epsilon(p)$ is obtained by solving

$$\frac{\epsilon + p}{p}\frac{\mathrm{d}p}{\mathrm{d}\epsilon} = \Gamma(p). \tag{3}$$

Truncating the spectral decomposition at four terms has been shown to produce reasonably good fits to realistic equations of state, including SLy [46].

The equation of state—and hence the set of parameters $\Upsilon = \{\gamma_0, \gamma_1, \gamma_2, \gamma_3\}$—determines how the tidal deformability depends on mass: $\Lambda(\Upsilon; m)$. The likelihood for the full set of data d given these parameters is

$$\mathcal{L}(d|\Upsilon) = \prod_{i=1}^{N} \int \mathrm{d}m_1^i \int \mathrm{d}m_2^i \pi(m_1^i, m_2^i) \times \mathcal{L}_\kappa(d_i|m_1^i, m_2^i, \Lambda(\Upsilon; m_1^i), \Lambda(\Upsilon; m_2^i)), \tag{4}$$

where $\mathcal{L}_\kappa(d_i|\cdots)$ are the single-event likelihoods. Meanwhile, $\pi(m_1^i, m_2^i)$ is the prior on the component masses, which we take to be the distribution from [36] used to simulate our population of binary neutron stars. We evaluate this marginal likelihood with a Riemann sum over bins a, b of each KDE $\mathcal{K}_i$:

$$\mathcal{L}(d|\Upsilon) \approx \prod_{i=1}^{N} \Delta m_1^i \Delta m_2^i \sum_{a,b} \pi(m_1^a, m_2^b) \times \mathcal{K}_i(m_1^a, m_2^b, \Lambda(\Upsilon; m_1^a), \Lambda(\Upsilon; m_2^b)). \tag{5}$$

The posterior probability is then

$$p(\Upsilon|d) \propto \mathcal{L}(d|\Upsilon)\pi(\Upsilon) \tag{6}$$

where we take the prior $\pi(\Upsilon)$ on the equation of state parameters to be uniform in the ranges $\gamma_0 \in [0.2, 2.0]$, $\gamma_1 \in [-1.6, 1.7]$, $\gamma_2 \in [-0.6, 0.6]$, and $\gamma_3 \in [-0.02, 0.02]$. This translates to a prior in the radius shown in Fig. 4.

III. RESULTS AND DISCUSSION

The 90% credible intervals for $p(\epsilon)$ and $R(m)$ are shown in Fig. 2. The different shading shows how the constraints vary depending on the number of events used in the fit: the 5 loudest (light), the 10 loudest (medium), and the 75 loudest (dark). The SLy equation of state used to generate the data is the dashed black curve. The dashed black curve is enclosed within the one-sigma credible interval, indicating that we successfully estimate the true equation of state.

The 75 loudest events allow us to constrain $R(m)$ to within an average of ~200 m over the interval 1–1.97$M_\odot$. The constraint is ~75 m around 1.4–1.6$M_\odot$, near where our distribution of binary neutron stars peaks. We constrain the pressure to within an average of ~18% in the energy density range $2 \times 10^{34} - 2 \times 10^{35}$ J m^{-3}. The constraint is ~4% at $\epsilon \approx 5.2 \times 10^{34}$ J m^{-3}.

Our ability to constrain the equation of state starts to plateau at around the first 20 loudest events. Including additional events improves the constraints, but with diminishing returns.

Figure 3 shows the width of the $R(m)$ credible interval as a function the number of loudest events, N_{loudest}, included in the analysis. The width shows little change beyond $N_{\mathrm{loudest}} \gtrsim 20$ for all values of the mass. We conclude that the loudest events play an outsize role constraining the equation of state. However, given the sheer volume of binary neutron star detections ($\approx 3 \times 10^5$ per year of Cosmic Explorer [6]), the effect of so many small

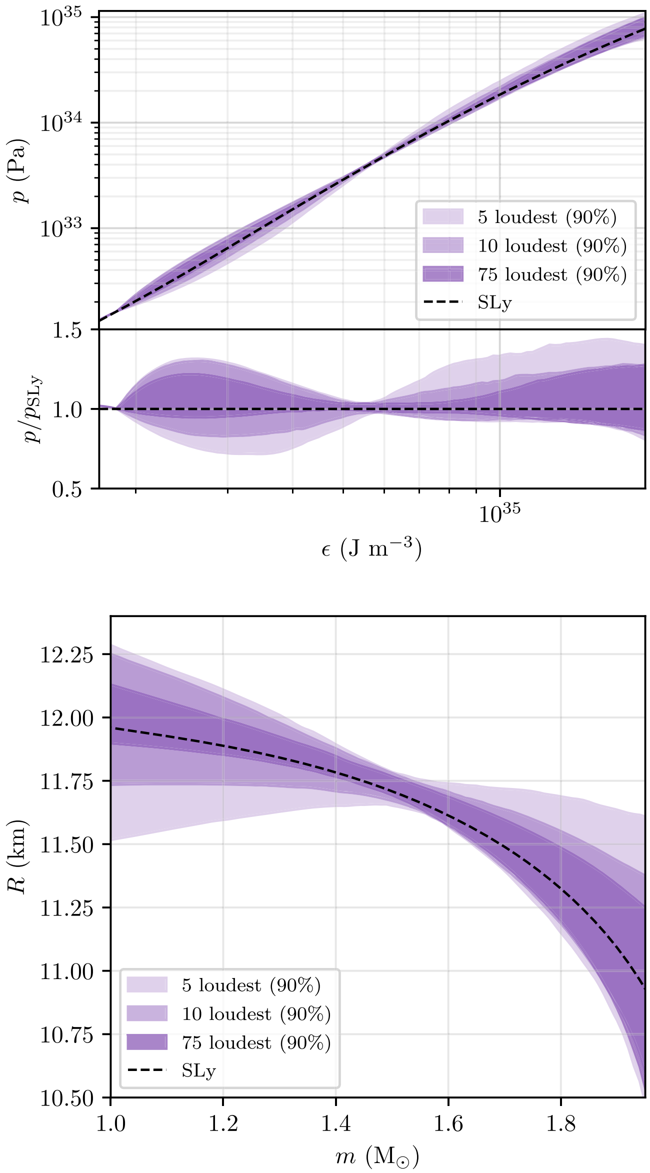

FIG. 2. Constraints on the neutron star equation of state. The shaded purple regions show the 90% credible intervals. The light contours are derived using only the 5 loudest events; the medium contours using the 10 loudest events; and the dark contours using the 75 loudest events. Top: pressure p as a function of energy density ϵ. The upper panel shows the pressure in units of Pa. The lower panel shows the pressure relative to the `SLy` equation of state used to generate the data. Bottom: the radius R as a function of mass m. In all three panels, the `SLy` curve is indicated with the dashed black curve.

improvements may become significant. Indeed, the curves are well-fit by both a decaying exponential and a power-law with exponent $-1/2$ (shown in the figure). The former predicts negligible improvement even with the full set of data, while the latter predicts an improvement by at least a factor of two. Our sensitivity estimates are therefore conservative. A mock study to estimate the sensitivity gained from including every binary neutron star detected by

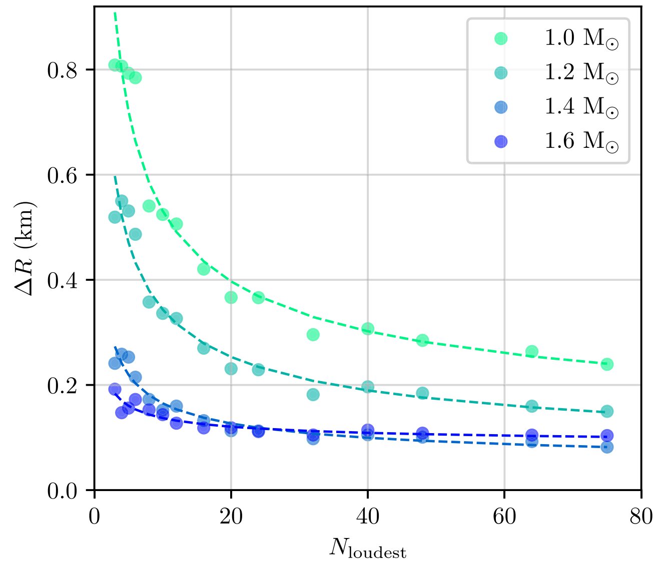

FIG. 3. The width of the 90% $R(m)$ credible interval as a function of the number of loudest events used in the analysis N_{loudest}. The relationship is well fit by a $1/\sqrt{N_{\mathrm{loudest}}}$ law that approaches a nonzero value at large N_{loudest}, as shown by the dashed curves. The improvement in the credible interval begins to diminish significantly beyond about $N_{\mathrm{loudest}} = 20$.

Cosmic Explorer and the Einstein Telescope would require significant computational resources.

Figure 3 shows the results for the 75 loudest events in one year of simulated data. The exact shape of this constraint will vary with each simulated dataset due to cosmic variance—random variation in the set of binary neutron stars. However, we expect this variance to be small compared to the statistical uncertainty.

These results are based on the `SLy` equation of state, but we expect them to be representative of the constraints achievable for any smooth equation of state that is well-fit by parametric models. To test this, we repeat the analysis using the `ALF2` model, which predicts larger tidal deformabilities and radii 1–2 km larger than `SLy`. The resulting constraints (Fig. 5) are not appreciably different from those reported above, with the average credible interval being only 2% smaller and the best constraint 10% smaller. However, while these results capture smooth equations of state, the true equation of state may not be so "nice" and could potentially exhibit discontinuous behavior in the speed of sound due to e.g. phase transitions [47,48]. This can result in uncertainties in derived quantities such as the radius being underreported when using smooth parametric models [49,50]. Next-generation x-ray pulse profile observations—such as those by the planned STROBE-X—will allow neutron star radii to be measured to $\sim 2\% - 4\%$ [51], providing a valuable check on the constraints from tidal deformability measurements using gravitational waves.

By adopting a zero-spin prior, we obtain a narrower mass posterior than we would if we allowed for non-zero spin. We test how this might affect our equation of state constraints by repeating the analysis using a uniform prior on the dimensionless spin parameter $\chi \in [-0.1, 0.1]$. Despite a significant broadening in the mass posterior, we find only a small difference in the constraints when using the uniform prior (see Figure 6), with the average credible interval being only 9% larger and the best constraint 17% larger. This suggests that for such precise measurements of the mass, the equation of state estimation is relatively insensitive to assumptions about neutron star spin.

IV. COMPARISON WITH CURRENT CONSTRAINTS

Observations of the binary neutron star merger GW170817 by LIGO-Virgo [52] constrained the neutron-star radius with a precision of 2.8 km at 90% credibility [4]. Our results therefore suggest that a network consisting of Cosmic Explorer + Einstein Telescope will improve on this constraint by a factor of $\gtrsim 10$ after 1 year of observations. The neutron star equation of state is also constrained by the Neutron Star Interior Composition Explorer (NICER) and X-ray Multi-Mirror (XMM-Newton) observatories, using fits to emission from rotating hot spots [53,54]. When the NICER and XMM-Newton measurements are combined with the tidal deformability constraints from GW170817 [4] and GW190425 [55], the radius at $1.4 M_\odot$ is constrained to 16% at 90% credibility [54,56,57] The constraint from third-generation gravitational-wave observatories will be $\lesssim 2\%$. Of course, in this work we include only the 75 loudest events detected in one year of data. The constraints obtained from the addition of hundreds of thousands of weaker events will improve the constraints by an unknown amount.

V. LIMITATIONS

There are some limitations with this analysis that are worthy of further investigation. The binary neutron star merger rate remains highly uncertain [52,58]. A higher merger rate at small redshift will result in an increased number of loud events. Since the constraint on the equation of state appears to be driven by the loudest sources, we expect such an enhanced merger rate to lead to a better constraint.

For this analysis we use a Gaussian approximation to the observed Galactic binary neutron star distribution. However, this is unlikely to be entirely representative of the extragalactic distribution, with measurements of GW190425 [55] suggesting a that the extragalactic distribution is broader [59].

It has been shown that a poorly chosen prior for the mass can bias the inferred equation of state [16]. We find no noticeable difference in the results even in the extreme case of a uniform prior in the component masses. This is expected in the case of measurements by third-generation observatories, since any non-pathological prior will vary little over the narrow range in mass on which the likelihood has support.

Finally, we note that these results are only as accurate as the waveforms used to produce the mock measurements. Such precise measurements require highly accurate waveforms to avoid mismodeling biases, potentially making the effects of additional resonant modes and higher post-Newtonian orders significant [60,61]. Recently, [21] has shown that including the effects of resonant r-modes in Einstein Telescope observations has a noticeable impact on the inferred equation of state.

ACKNOWLEDGMENTS

We thank Paul Lasky, Aditya Vijaykumar, Ling Sun, Isaac Legred, and Tathagata Ghosh for helpful comments. This work is supported by the Australian Research Council (ARC) through the Centre of Excellence for Gravitational Wave Discovery (OzGrav) Projects CE170100004 and CE230100016, Discovery Project DP230103088, and LIEF Project No. LE210100002. This work was performed on the OzSTAR national facility at Swinburne University of Technology. The OzSTAR program receives funding in part from the Astronomy National Collaborative Research Infrastructure Strategy (NCRIS) allocation provided by the Australian Government, and from the Victorian Higher Education State Investment Fund (VHESIF) provided by the Victorian Government.

APPENDIX

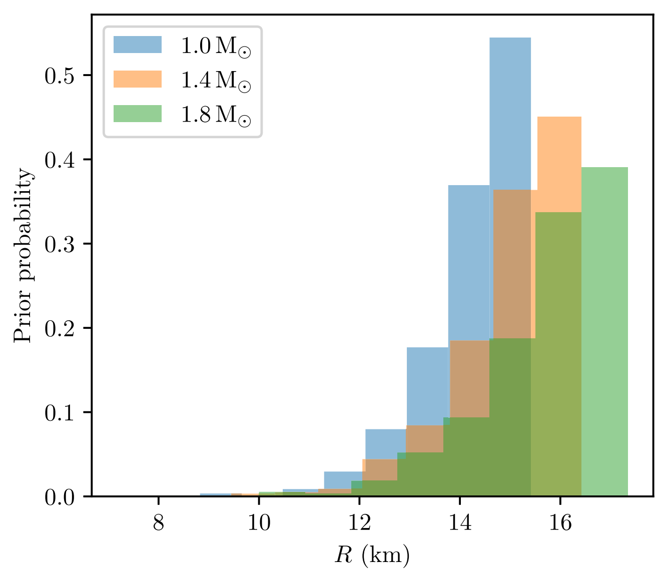

FIG. 4. Radius priors used for hyperparameter estimation of the spectral parameters.

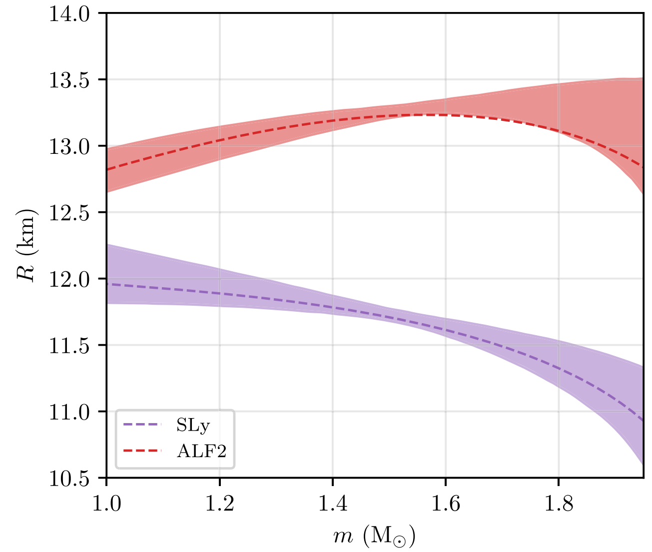

FIG. 5. Constraint on an ALF2 (red) and an SLy (purple) equation of state using the same 16 events.

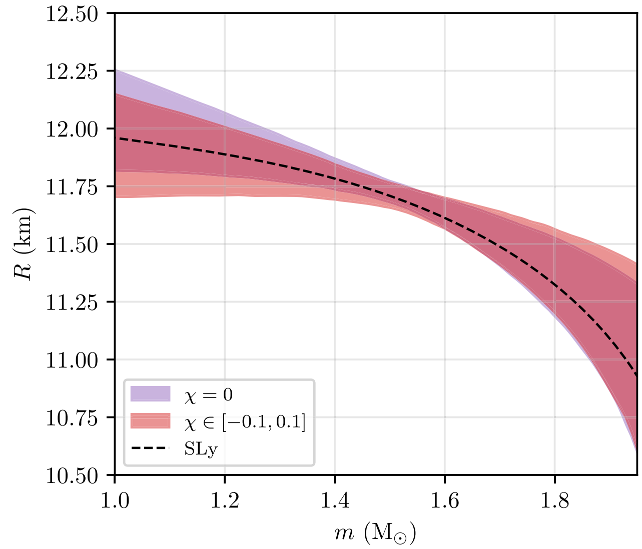

FIG. 6. Constraint on the SLy equation of state using a prior in the dimensionless spin χ fixed at zero (purple) and uniform in the range $[-0.1, 0.1]$ (red).

[1] G. F. Burgio, H. J. Schulze, I. Vidaña, and J. B. Wei, Neutron stars and the nuclear equation of state, Prog. Part. Nucl. Phys. **120**, 103879 (2021).
[2] H. Yu, N. N. Weinberg, P. Arras, J. Kwon, and T. Venumadhav, Beyond the linear tide: Impact of the nonlinear tidal response of neutron stars on gravitational waveforms from binary inspirals, Mon. Not. R. Astron. Soc. **519**, 4325 (2023).
[3] A "stiffer" equation of state implies that the neutron star is more resistant to contraction under the influence of its own gravity, and so stiffer equations of state tend to produce relatively larger neutron stars than soft equations of state.
[4] B. P. Abbott *et al.* (The LIGO Scientific and the Virgo Collaborations), GW170817: Measurements of neutron star radii and equation of state, Phys. Rev. Lett. **121**, 161101 (2018).
[5] D. Radice, A. Perego, F. Zappa, and S. Bernuzzi, GW170817: Joint constraint on the neutron star equation of state from multimessenger observations, Astrophys. J. Lett. **852**, L29 (2018).
[6] M. Evans *et al.*, A horizon study for cosmic explorer: Science, observatories, and community, arXiv:2109.09882.
[7] B. P. Abbott *et al.* (The LIGO Scientific Collaboration), Exploring the sensitivity of next generation gravitational wave detectors, Classical Quantum Gravity **34**, 044001 (2017).
[8] D. Reitze *et al.*, Cosmic Explorer: The U.S. contribution to gravitational-wave astronomy beyond LIGO, Bull. Am. Astron. Soc. **51**, 035 (2019), https://baas.aas.org/pub/2020n7i035.
[9] M. Punturo *et al.*, The third generation of gravitational wave observatories and their science reach, Classical Quantum Gravity **27**, 084007 (2010).
[10] S. Hild *et al.*, Sensitivity studies for third-generation gravitational wave observatories, Classical Quantum Gravity **28**, 094013 (2011).
[11] M. Maggiore *et al.*, Science case for the Einstein telescope, J. Cosmol. Astropart. Phys. 03 (2020) 050.
[12] C. Markakis, J. S. Read, M. Shibata, K. Uryu, J. D. E. Creighton, and J. L. Friedman, Inferring the neutron star equation of state from binary inspiral waveforms, in *Twelfth Marcel Grossmann Meeting on General Relativity*, edited by A. H. Chamseddine (2012), pp. 743–745, arXiv:1008.1822.
[13] W. Del Pozzo, T. G. F. Li, M. Agathos, C. Van Den Broeck, and S. Vitale, Demonstrating the feasibility of probing the neutron-star equation of state with second-generation gravitational-wave detectors, Phys. Rev. Lett. **111**, 071101 (2013).
[14] L. Wade, J. D. E. Creighton, E. Ochsner, B. D. Lackey, B. F. Farr, T. B. Littenberg, and V. Raymond, Systematic and statistical errors in a Bayesian approach to the estimation of the neutron-star equation of state using advanced gravitational wave detectors, Phys. Rev. D **89**, 103012 (2014).
[15] B. D. Lackey and L. Wade, Reconstructing the neutron-star equation of state with gravitational-wave detectors from a realistic population of inspiralling binary neutron stars, Phys. Rev. D **91**, 043002 (2015).
[16] M. Agathos, J. Meidam, W. Del Pozzo, T. G. F. Li, M. Tompitak, J. Veitch, S. Vitale, and C. Van Den Broeck, Constraining the neutron star equation of state with gravitational wave signals from coalescing binary neutron stars, Phys. Rev. D **92**, 023012 (2015).
[17] K. Hotokezaka, K. Kyutoku, Y.-i. Sekiguchi, and M. Shibata, Measurability of the tidal deformability by

gravitational waves from coalescing binary neutron stars, Phys. Rev. D **93**, 064082 (2016).
[18] P. Kumar, M. Pürrer, and H. P. Pfeiffer, Measuring neutron star tidal deformability with Advanced LIGO: A Bayesian analysis of neutron star-black hole binary observations, Phys. Rev. D **95**, 044039 (2017).
[19] F. Hernandez Vivanco, R. Smith, E. Thrane, P. D. Lasky, C. Talbot, and V. Raymond, Measuring the neutron star equation of state with gravitational waves: The first forty binary neutron star merger observations, Phys. Rev. D **100**, 103009 (2019).
[20] C. Pacilio, A. Maselli, M. Fasano, and P. Pani, Ranking love numbers for the neutron star equation of state: The need for third-generation detectors, Phys. Rev. Lett. **128**, 101101 (2022).
[21] P. K. Gupta, A. Puecher, P. T. H. Pang, J. Janquart, G. Koekoek, and C. V. D. Broeck, Determining the equation of state of neutron stars with einstein telescope using tidal effects and r-mode excitations from a population of binary inspirals, arXiv:2205.01182.
[22] R. Huxford, R. Kashyap, S. Borhanian, A. Dhani, and B. S. Sathyaprakash, The accuracy of neutron star radius measurement with the next generation of terrestrial gravitational-wave observatories, Phys. Rev. D **109**, 103035 (2024).
[23] B. K. Pradhan, D. Pathak, and D. Chatterjee, Constraining nuclear parameters using gravitational waves from f-mode oscillations in neutron stars, Astrophys. J. **956**, 38 (2023).
[24] T. Ghosh, B. Biswas, and S. Bose, Simultaneous inference of neutron star equation of state and the Hubble constant with a population of merging neutron stars, Phys. Rev. D **106**, 123529 (2022).
[25] D. Finstad, L. V. White, and D. A. Brown, Prospects for a precise equation of state measurement from Advanced LIGO and cosmic explorer, Astrophys. J. **955**, 45 (2023).
[26] B. K. Pradhan, T. Ghosh, D. Pathak, and D. Chatterjee, Cost of inferred nuclear parameters towards the f-mode dynamical tide in binary neutron stars, Astrophys. J. **966**, 79 (2024).
[27] M. Vallisneri, Use and abuse of the fisher information matrix in the assessment of gravitational-wave parameter-estimation prospects, Phys. Rev. D **77**, 042001 (2008).
[28] R. Smith, S. E. Field, K. Blackburn, C.-J. Haster, M. Pürrer, V. Raymond, and P. Schmidt, Fast and accurate inference on gravitational waves from precessing compact binaries, Phys. Rev. D **94**, 044031 (2016).
[29] W. Althouse, L. Jones, and A. Lazzarini, Determination of global and local coordinate axes for the LIGO sites, Technical Report LIGO-T980044-10, LIGO, 2001.
[30] M. Safarzadeh, E. Berger, K. K. Y. Ng, H.-Y. Chen, S. Vitale, C. Whittle, and E. Scannapieco, Measuring the delay time distribution of binary neutron stars. II. Using the redshift distribution from third-generation gravitational-wave detectors network, Astrophys. J. **878**, L13 (2019).
[31] M. Burgay, N. D'Amico, A. Possenti, R. N. Manchester, A. G. Lyne, B. C. Joshi, M. A. McLaughlin, M. Kramer, J. M. Sarkissian, F. Camilo, V. Kalogera, C. Kim, and D. R. Lorimer, An increased estimate of the merger rate of double neutron stars from observations of a highly relativistic system, Nature (London) **426**, 531 (2003).
[32] K. Stovall *et al.*, PALFA discovery of a highly relativistic double neutron star binary, Astrophys. J. Lett. **854**, L22 (2018).
[33] B. P. Abbott *et al.* (LIGO Scientific and Virgo Collaborations), Properties of the binary neutron star merger GW170817, Phys. Rev. X **9**, 011001 (2019).
[34] I. Harry and T. Hinderer, Observing and measuring the neutron-star equation-of-state in spinning binary neutron star systems, Classical Quantum Gravity **35**, 145010 (2018).
[35] D. Wysocki, R. O'Shaughnessy, L. Wade, and J. Lange, Inferring the neutron star equation of state simultaneously with the population of merging neutron stars, arXiv:2001.01747.
[36] B. Kiziltan, A. Kottas, M. De Yoreo, and S. E. Thorsett, The neutron star mass distribution, Astrophys. J. **778**, 66 (2013).
[37] N. Farrow, X.-J. Zhu, and E. Thrane, The mass distribution of galactic double neutron stars, Astrophys. J. **876**, 18 (2019).
[38] F. Douchin and P. Haensel, A unified equation of state of dense matter and neutron star structure, Astron. Astrophys. **380**, 151 (2001).
[39] LIGO Scientific Collaboration, LIGO Algorithm Library—LALSuite, free software (GPL), 10.7935/GT1W-FZ16 (2018).
[40] E. Higson, W. Handley, M. Hobson, and A. Lasenby, Dynamic nested sampling: An improved algorithm for parameter estimation and evidence calculation, Stat. Comput. **29**, 891 (2018).
[41] G. Ashton *et al.*, BILBY: A user-friendly Bayesian inference library for gravitational-wave astronomy, Astrophys. J. **241**, 27 (2019).
[42] I. M. Romero-Shaw *et al.*, Bayesian inference for compact binary coalescences with BILBY: Validation and application to the first LIGO-Virgo gravitational-wave transient catalogue, Mon. Not. R. Astron. Soc. **499**, 3295 (2020).
[43] R. J. E. Smith, G. Ashton, A. Vajpeyi, and C. Talbot, Massively parallel Bayesian inference for transient gravitational-wave astronomy, Mon. Not. R. Astron. Soc. **498**, 4492 (2020).
[44] R. Smith *et al.*, Bayesian inference for gravitational waves from binary neutron star mergers in third generation observatories, Phys. Rev. Lett. **127**, 081102 (2021).
[45] Experimentation with other kernels suggests that our results are robust to the choice of kernel.
[46] L. Lindblom, Spectral representations of neutron-star equations of state, Phys. Rev. D **82**, 103011 (2010).
[47] P. Landry and R. Essick, Nonparametric inference of the neutron star equation of state from gravitational wave observations, Phys. Rev. D **99**, 084049 (2019).
[48] C. A. Raithel and E. R. Most, Tidal deformability doppelgänger: Implications of a low-density phase transition in the neutron star equation of state, Phys. Rev. D **108**, 023010 (2023).
[49] I. Legred, K. Chatziioannou, R. Essick, and P. Landry, Implicit correlations within phenomenological parametric models of the neutron star equation of state, Phys. Rev. D **105**, 043016 (2022).
[50] I. Legred, B. O. Sy-Garcia, K. Chatziioannou, and R. Essick, Assessing equation of state-independent relations

for neutron stars with nonparametric models, Phys. Rev. D **109**, 023020 (2024).
[51] P. S. Ray *et al.*, Strobe-x: X-ray timing and spectroscopy on dynamical timescales from microseconds to years, arXiv:1903.03035.
[52] B. P. Abbott *et al.*, GW170817: Observation of gravitational waves from a binary neutron star inspiral, Phys. Rev. Lett. **119**, 161101 (2017).
[53] M. C. Miller *et al.*, PSR J0030 + 0451 mass and radius from NICER data and implications for the properties of neutron star matter, Astrophys. J. Lett. **887**, L24 (2019).
[54] M. C. Miller *et al.*, The radius of PSR J0740 + 6620 from NICER and XMM-Newton data, Astrophys. J. Lett. **918**, L28 (2021).
[55] B. P. Abbott, GW190425: Observation of a compact binary coalescence with total mass $\sim 3.4 M_{\odot}$, Astrophys. J. **892**, L3 (2020).
[56] G. Raaijmakers, S. K. Greif, K. Hebeler, T. Hinderer, S. Nissanke, A. Schwenk, T. E. Riley, A. L. Watts, J. M. Lattimer, and W. C. G. Ho, Constraints on the dense matter equation of state and neutron star properties from NICER's mass-radius estimate of PSR J0740 + 6620 and multimessenger observations, Astrophys. J. Lett. **918**, L29 (2021).
[57] P. T. H. Pang, I. Tews, M. W. Coughlin, M. Bulla, C. Van Den Broeck, and T. Dietrich, Nuclear physics multimessenger astrophysics constraints on the neutron star equation of state: Adding NICER's PSR J0740 + 6620 measurement, Astrophys. J. **922**, 14 (2021).
[58] C. Kim, B. B. P. Perera, and M. A. McLaughlin, Implications of PSR J0737-3039B for the Galactic NS-NS binary merger rate, Mon. Not. R. Astron. Soc. **448**, 928 (2015).
[59] P. Landry and J. S. Read, The mass distribution of neutron stars in gravitational-wave binaries, Astrophys. J. Lett. **921**, L25 (2021).
[60] C. B. Owen, C.-J. Haster, S. Perkins, N. J. Cornish, and N. Yunes, Waveform accuracy and systematic uncertainties in current gravitational wave observations, Phys. Rev. D **108**, 044018 (2023).
[61] Q. Hu and J. Veitch, Assessing the model waveform accuracy of gravitational waves, Phys. Rev. D **106**, 044042 (2022).